Cooperative interactions of BRAF^{V600E} kinase and *CDKN2A* locus deficiency in pediatric malignant astrocytoma as a basis for rational therapy

Emmanuelle Huillard[a,b,1,2], Rintaro Hashizume[c,1], Joanna J. Phillips[c,d], Amélie Griveau[a,b], Rebecca A. Ihrie[b,c,3], Yasuyuki Aoki[c], Theodore Nicolaides[a,c], Arie Perry[c,d], Todd Waldman[e], Martin McMahon[f], William A. Weiss[a,c,g], Claudia Petritsch[c], C. David James[c,4], and David H. Rowitch[a,b,c,4]

Departments of [a]Pediatrics, [c]Neurological Surgery, [g]Neurology, and [d]Neuropathology, [b]Eli and Edyth Broad Institute for Stem Cell Research and Regeneration Medicine and Howard Hughes Medical Institute, and [f]Department of Cellular and Molecular Pharmacology, Helen Diller Family Comprehensive Cancer Center, University of California, San Francisco, CA 94143; and [e]Department of Oncology, Lombardi Comprehensive Cancer Center, Georgetown University, Washington, DC 20057

Edited by Webster K. Cavenee, Ludwig Institute, University of California San Diego, La Jolla, CA, and approved April 16, 2012 (received for review October 25, 2011)

Although malignant astrocytomas are a leading cause of cancer-related death in children, rational therapeutic strategies are lacking. We previously identified activating mutations of v-raf murine sarcoma viral oncogene homolog B1 (*BRAF*) (*BRAF^{T1799A}* encoding BRAF^{V600E}) in association with homozygous cyclin-dependent kinase inhibitor 2A (*CDKN2A*, encoding *p14ARF* and *p16Ink4a*) deletions in pediatric infiltrative astrocytomas. Here we report that BRAF^{V600E} expression in neural progenitors (NPs) is insufficient for tumorigenesis and increases NP cellular differentiation as well as apoptosis. In contrast, astrocytomas are readily generated from NPs with additional *Ink4a-Arf* deletion. The BRAF^{V600E} inhibitor PLX4720 significantly increased survival of mice after intracranial transplant of genetically relevant murine or human astrocytoma cells. Moreover, combination therapy using PLX4720 plus the Cyclin-dependent kinase (CDK) 4/6-specific inhibitor PD0332991 further extended survival relative to either monotherapy. Our findings indicate a rational therapeutic strategy for treating a subset of pediatric astrocytomas with *BRAF^{V600E}* mutation and *CDKN2A* deficiency.

glioma | protein kinase | tumor suppressor

The incidence of pediatric central nervous system (CNS) tumors is second only to leukemia among malignancies affecting children (1). Among these tumors, malignant astrocytoma, including anaplastic astrocytoma World Health Organization (WHO) grade III and glioblastoma WHO grade IV, is a leading cause of mortality. However, development of rational targeted therapies for pediatric malignant astrocytoma has been limited by inadequate information regarding the relevant underlying genetic alterations and their signaling pathway consequences. In adults, glioblastomas (GBMs) have been categorized into subtypes on the basis of gene expression patterns (2, 3) and mutations affecting core RAS, PI3-kinase, TP53, and pRB signaling pathways (4). The spectrum and frequency of mutations in pediatric malignant astrocytoma, however, differ from that in adults. For example, whereas mutations and amplifications of *EGFR* are common in adult glioblastomas (GBM), they are observed only rarely in corresponding pediatric anaplastic astrocytomas or GBM (5–10). Similarly, mutations of *PTEN* and *IDH1* are relatively uncommon in pediatric astrocytomas (5). Recent studies have reported recurrent mutations of histone H3 and chromatin remodeling genes in pediatric GBM (6, 7).

Previously, we used a whole genome approach to identify copy number variance and mutations in pediatric astrocytomas (11). This analysis revealed activating mutations of v-raf murine sarcoma viral oncogene homolog B1 (*BRAF*) (*BRAF^{T1799A}* encoding BRAF^{V600E}) in 7/31 (23%) cases of pediatric diffuse astrocytoma (WHO grades II–IV), consistent with subsequent findings from others, and is in contrast to adult GBMs, which infrequently show *BRAF^{V600E}* mutation (12, 13). In our series, *BRAF^{T1799A}* occurred coincident with homozygous deletion of cyclin-dependent kinase inhibitor 2A (*CDKN2A*), encoding *Ink4a-Arf* in 5/7 cases (71%), suggesting the possibility of mechanistic cooperation between these two alterations in promoting glial tumor malignancy.

Here we investigated genetic requirements for generation of malignant astrocytomas in mice and used this information in preclinical testing. We show that expression of *BRAF^{V600E}* mutation in combination with homozygous *CDKN2A*/*Ink4a-Arf* deletion is sufficient for formation of tumors with histology typical of malignant astrocytomas in humans. Further, we have used this mouse model, as well as human malignant astrocytoma xenografts with genetically faithful *BRAF^{V600E}* and *Ink4a-Arf* mutations, to test a unique therapeutic strategy. We report that combination therapy with BRAF^{V600E} and Cyclin-dependent kinase (CDK) 4/6 inhibitors has remarkable activity against intracranial tumors in vivo. Together our data suggest that it is possible to faithfully model the genetics of a subset of pediatric malignant astrocytomas in mice and to use combined murine and human tumor models as platforms for testing rational therapies.

Results

Strategy for Faithful Regulation of BRAF^{V600E} Expression in Mouse Neural Progenitor Cells to Model Pediatric Malignant Astrocytoma. To precisely model activating mutations of *BRAF* found in pediatric astrocytomas, we used *Braf^{CA}* mice carrying a genetically engineered knock-in allele of *Braf* (14). The *Braf^{CA}* allele expresses normal Braf in its nonrecombined configuration. However, upon exposure to bacteriophage P1 cre recombinase, the *Braf^{CA}* allele is recombined to encode mutationally activated BRAF^{V600E} at normal physiological levels of expression. By using the *Braf^{CA}* allele in a heterozygous configuration, we precisely mimic the status of heterozygous *BRAF* mutations in human

Author contributions: E.H., R.H., R.A.I., C.P., C.D.J., and D.H.R. designed research; E.H., R.H., J.J.P., A.G., R.A.I., Y.A., and C.P. performed research; T.N., T.W., and M.M. contributed new reagents/analytic tools; E.H., R.H., J.J.P., T.N., A.P., T.W., M.M., W.A.W., C.D.J., and D.H.R. analyzed data; and E.H., R.H., C.D.J., and D.H.R. wrote the paper.

The authors declare no conflict of interest.

This article is a PNAS Direct Submission.

Freely available online through the PNAS open access option.

[1]E.H. and R.H. contributed equally to this work.

[2]Present address: Université Pierre et Marie Curie S975/Institut National de la Santé et de la Recherche Médicale U975/Centre National de la Recherche Scientifique UMR7225, Centre de Recherche de l'Institut du Cerveau et de la Moelle Epinière, 75651 Paris Cedex 13, France.

[3]Present address: Vanderbilt University Medical Center, Nashville, TN 37232-6840.

[4]To whom correspondence may be addressed. E-mail: david.james@ucsf.edu or rowitchd@peds.ucsf.edu.

This article contains supporting information online at www.pnas.org/lookup/suppl/doi:10.1073/pnas.1117255109/-/DCSupplemental.

pediatric tumors (11). We considered this strategy more accurate for investigating the expression of $BRAF^{V600E}$ than introduction by lentivirus, in which case the expression of a single splice variant of mutated *BRAF* would be driven by a strong viral promoter that is not subject to regulation by the factors involved in control of endogenous BRAF expression in normal or malignant cells. Indeed, the importance of faithful $BRAF^{V600E}$ regulation is indicated by other recent studies (14–17).

To assess whether *BRAF* activation alone is sufficient for tumor formation from neural progenitors (NPs), we crossed $Braf^{CA/+}$ hemizygous mice to *hGFAP-cre* transgenic mice expressing cre under the control of the *hGFAP* promoter, which targets neural stem cells and astroglia in the developing brain (18). The resulting *hGFAP-cre;* $Braf^{CA}$ compound heterozygous mice displayed an enlarged brain with expanded populations of type A neuroblasts in the subventricular zone, oligodendrocytes, and astroglia. Such animals survived until approximately 3 wk of age but did not demonstrate evidence of tumor development in the brain. Because of the lethality associated with $BRAF^{V600E}$ expression in these transgenic mice, we used an alternative system of orthotopic transplant of tumorigenic progenitor cells harvested from embryonic ventral telencephalon (Fig. 1*A*) (19, 20). *hGFAP-cre;* $Braf^{CA/+}$ NPs were harvested and expanded for transplant into SCID mice by intracranial injection. In this experimental paradigm, mice undergo injection of 2×10^5 dissociated NP cells and are then monitored for symptoms indicative of tumor development. As shown in Table 1, of five mice injected with cells expressing $BRAF^{V600E}$ alone, we observed no evidence of gross or microscopic tumor formation after 6 mo. We obtained similar results with NP cells derived from *Olig2-cre;* $Braf^{CA/+}$ mice ($n = 6$, Table 1).

$BRAF^{V600E}$ Expression in Combination with *Ink4a-Arf* Loss of Function Is Sufficient for Tumorigenesis. $Braf^{CA/+}$ mice were then crossed with mice lacking *Ink4a-Arf* to test the influence of $p16^{Ink4a}$ and $p19^{Arf}$ tumor suppressor function. In contrast to the findings above, expression of $BRAF^{V600E}$ in *Ink4a-Arf*–deficient neurospheres (line 10740) was associated with tumor formation 3–4 mo after intracranial implantation (Table 1 and Fig. 1*B*). We obtained comparable results in SCID mice injected with identical $Braf^{CA/+}$; *Ink4a-Arf*$^{-/-}$ cells infected with an adenovirus encoding cre (Ad-cre; line 10776) (Table 1 and Fig. 1*B*). These findings indicate that expression of $BRAF^{V600E}$ cooperates with *Ink4a-Arf* deletion in tumor formation. Our results do not rule out the possibility of tumor formation at later time points, but nonetheless suggest that expression of $BRAF^{V600E}$ alone is insufficient to confer tumorigenicity to NPs.

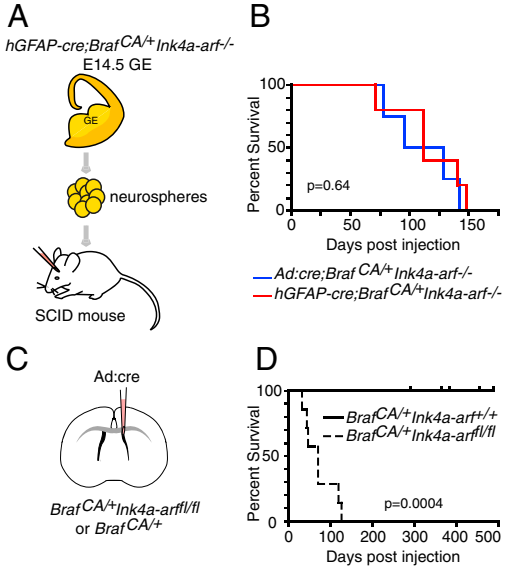

Fig. 1. Concurrent $BRAF^{V600E}$ activation and *Ink4a-arf* deletion induces malignant astrocytoma from mouse neural progenitors. (*A*) Mouse model for pediatric malignant astrocytoma. GE, ganglionic eminence; ctx, cortex. (*B*) Kaplan–Meier survival curves of SCID mice transduced with *hGFAP-cre* $Braf^{CA/+}$ *Ink4a-Arf*$^{-/-}$ ($n = 6$) or Ad:cre $Braf^{CA/+}$ *Ink4a-Arf*$^{-/-}$ ($n = 5$) neural progenitor cells ($P = 0.64$). (*C*) Injection of an adenovirus encoding ubiquitous cre expression into $Braf^{CA/+}$ or $Braf^{CA/+}$ *Ink4a-arf*$^{LoxP/LoxP}$ adult mice. (*D*) Kaplan–Meier survival curves of $Braf^{CA/+}$ ($n = 6$) and $Braf^{CA/+}$ *Ink4a-arf*$^{LoxP/LoxP}$ ($n = 9$) mice injected with Ad:cre into the lateral ventricle ($P = 0.0004$).

Tumors exhibited restricted infiltration and tended to grow exophytically despite high mitotic index, nuclear pleomorphism, and expression of cellular markers typical of human pediatric astrocytoma, including Olig2, GFAP, and Nestin (21) (Fig. S1). Lines 10740 and 10776 were further manipulated by introduction of a luciferase reporter to allow noninvasive bioluminescence imaging (BLI). After passage in the murine brain, the tumors took on a highly infiltrative growth pattern characteristic of malignant astrocytoma with diffuse invasion throughout the cerebral hemisphere and extension along white matter tracts (see Fig. 4*A*). Tumor cells exhibited marked pleomorphism, had a high mitotic index, and expressed phosphorylated ERK (Fig. S2), which is an expected downstream consequence of BRAF activation. Because line 10776 demonstrated invasive histology and robustly expressed markers typical of pediatric astrocytoma including Olig2 (21), it was prioritized for further study.

To further investigate cooperative interactions between $BRAF^{V600E}$ expression and *Ink4a-Arf* deletion, we injected Ad:cre into the subventricular zone of mice carrying $Braf^{CA/+}$ alone or $Braf^{CA/+}$; *Ink4a-arf*$^{fl/fl}$ (Fig. 1*C*). No tumor formation was observed following injections of $Braf^{CA/+}$ mice for up to 490 d postinjection (Fig. 1*D* and Table 1). In contrast, intracranial tumor formation was observed in all $Braf^{CA/+}$ *Ink4a-arf*$^{fl/fl}$ mice injected with Ad:cre (median survival, 70 d). These findings indicate that heterozygous $BRAF^{V600E}$ expression alone is insufficient to promote tumor development in vivo. In contrast, such $BRAF^{V600E}$ expression is transforming when combined with homozygous inactivation of *Ink4a-Arf*.

$BRAF^{V600E}$ Mutation Combined with *Ink4a-Arf* Deletion Results in Reduced Differentiation and Apoptosis, as Well as Enhanced Proliferation of Neural Progenitors. To further investigate the apparent cooperativity of $BRAF^{V600E}$ and *Ink4a-Arf* mutations, we cultured NPs that harbored these mutations. As shown in Fig. 2, *hGFAP-cre;* $Braf^{CA/+}$; *Ink4a-Arf*$^{-/-}$ cells have an increased proportion of bromodeoxyuridine (BrdU) positivity and a decreased apoptotic fraction compared with cells with intact $p16^{Ink4a}$. Moreover, $Braf^{CA/+}$ cells lacking *Ink4a-Arf* have an impaired capacity to differentiate into neurons, oligodendrocytes, and astrocytes. Indeed, rather than differentiate, these cells proliferate even when subjected to differentiation culture conditions, as shown by their high Ki67-proliferative labeling indices (Fig. 2 *C* and *D*).

CDK4/6 Activity Is Required for Cell Cycle Progression of $BRAF^{V600E}$; *Ink4a-Arf*$^{-/-}$ Murine Astrocytoma Cells. p16 suppresses the activity of CDK4 and CDK6, which in turn antagonize retinoblastoma 1 (RB) activity to promote cell cycle progression. PD0332991 is an orally administered CDK4/6 inhibitor in clinical trials to assess efficacy against several types of cancer (22). We decided to test whether elevated CDK4/6 activity is necessary to sustain cell cycle progression in $BRAF^{V600E}$; *Ink4a-Arf*$^{-/-}$ NP cells. PD0332991 treatment significantly reduced BrdU incorporation and increased the G1 phase fraction of $BRAF^{V600E}$ NP cells that were *Ink4a-Arf*$^{-}$ null, but not *Ink4a-Arf* intact (Fig. 3 *A* and *B*), suggesting that sustained CDK4/6 activity is necessary for cell cycle progression. Use of ImageJ to analyze and compare phosphorylated Rb (pRb) band intensity in treated vs. untreated cells, for replicate experiments and multiple Western blot analyses, consistently revealed 50–80% decrease in pRb for PD0332991-treated *Ink4a-Arf*$^{-/-}$ cells, relative to untreated *Ink4a-Arf*$^{-/-}$ cells, and

MEDICAL SCIENCES

Table 1. Summary of the orthotopic transplants of murine cells and in vivo injections

	Genotype	No. of cell lines injected	No. of animals injected	% developing tumors	Median survival, d
Cell lines	*hGFAP-cre;BrafV600Efl/+*	2	5	0 (0/5)	ND*
	hGFAP-cre;BrafV600Efl/+ Ink4a-Arf$^{-/-}$	1	6	67 (4/6)	112
	Olig2-Cre;BrafV600Efl/+	2	6	0 (0/6)†	ND*
	Ad:cre;*BrafV600Efl/+ Ink4a-Arf*$^{-/-}$	2	4	100 (4/4)	112
	Ad:cre;*BrafV600Efl/+ Ink4a-Arf*$^{-/-}$ (10776)-luc	1	10	100 (10/10)	23
Ad:Cre injections	Adult *BrafV600Efl/+*	—	6	0 (0/6)	—
	Adult *BrafV600Efl/+ Ink4a-Arffl/fl*	—	9	100 (9/9)	70

*Mice were killed at 180 d postinjection and did not show signs of tumor or hyperplasia.
†Three mice were killed at 86–163 d postinjection and did not show signs of tumor or hyperplasia.

following normalization of pRb signal against either corresponding total Rb or β-tubulin signal. Representative immunoblot results are shown in Fig. 3*C*.

Dual BRAF^{V600E} and CDK4/6 Inhibition Shows Additive Effects Against Murine 10776 Astrocytoma Progenitors in Vivo. PLX4720 is a tool compound of the PLX4032 inhibitor, which has yielded encouraging clinical results in patients with BRAF^{V600E} metastatic melanoma (23). We found significant therapeutic benefit of PLX4720 monotherapy against murine 10776 astrocytoma, as indicated by bioluminescence monitoring and survival of treated mice (Fig. 4 *B* and *C*). Similarly, PD0332991 monotherapy provided a significant benefit (Fig. 4 *B* and *C*). To determine possible additive antitumor activity, a treatment group was included to evaluate PLX4720 + PD0332991 combination therapy. Bioluminescence monitoring of this treatment group showed further reduction of intracranial tumor growth rate, relative to either monotherapy (Fig. 4*B*), as well as increased survival benefit (Fig. 4*C*). Analysis of intratumor Ki67 staining showed reduced proliferation in mono and dual PLX4720- and PD0332991-treated samples compared with control tumors (Fig. 4 *D* and *E*). There were significantly fewer Ki67^{+} cells in the samples treated with the combination therapy compared with either monotherapy.

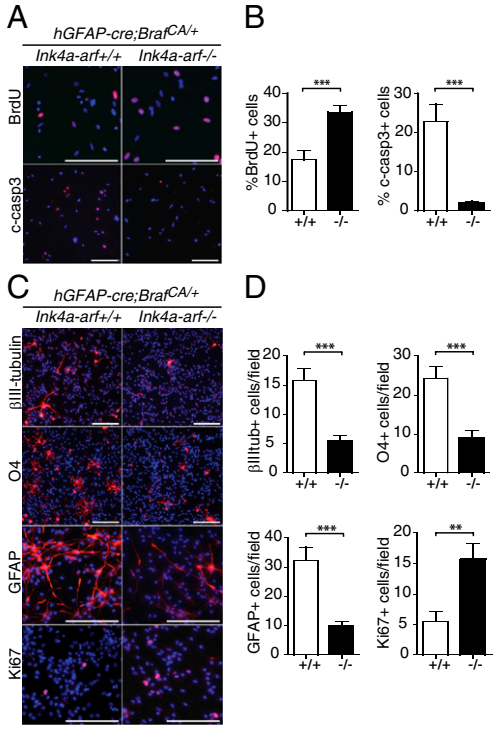

Fig. 2. *hGFAP-cre; Braf$^{CA/+}$Ink4a-Arf$^{-/-}$* cells are more proliferative and less differentiated than *hGFAP-cre; Braf$^{CA/+}$* cells. (*A*) Immunocytochemical analysis of proliferation (BrdU) and apoptosis (cleaved caspase 3) markers in *Braf$^{CA/+}$* and *Braf$^{CA/+}$ Ink4a-Arf$^{-/-}$* neural progenitors cultures. (Scale bars, 100 μm.) (*B*) Quantification of the numbers of BrdU^{+} and Cleaved-caspase 3^{+} cells. (*C*) Corresponding analysis of the differentiation markers βIII-tubulin (neuronal), GFAP (astrocyte), O4 (oligodendrocyte), and the proliferation marker Ki67 in neural progenitor cultures under differentiation culture conditions. (Scale bars, 100 μm.) (*D*) Quantification of the numbers of cells expressing the differentiation markers (mean ± SEM). ***$P < 0.0005$, **$P < 0.005$.

Human GBM Cell Line with *BRAF^{V600E}* Mutation and Deletion of *CDKN2A* Responds to Dual Inhibitor Therapy. We next extended results to a human malignant astrocytoma xenograft model, which used intracranial xenografts of the DBTRG05-MG astrocytoma cell line, previously determined as harboring BRAF^{V600E} (24), and for which we subsequently detected homozygous deletion of *CDKN2A* (25). As with the 10776 cells, DBTRG05-MG cells were modified with luciferase to enable bioluminescence monitoring. DBTRG05-MG xenografts showed features of high-grade astrocytoma, such as invasion, anaplastic tumor cell morphology, Nestin expression, and high mitotic index (Fig. 5*A*). Consistent with results obtained with the murine allograft model, we found that treatment of DBTRG05-MG tumors with each monotherapy resulted in reduced tumor growth rate and conferred substantial survival benefit, and combination therapy significantly outperformed either monotherapy (Fig. 5 *B* and *C*). Results from the analysis of tumor Ki67 positivity also revealed consistency with those obtained with the murine model: all therapies significantly reduced malignant astrocytoma xenograft cell proliferation relative to the vehicle treatment group (Fig. 5*D*). The treatment of a second human glioma line, AM-38, also showed combination therapy as being most effective at inhibiting tumor growth and extending animal survival (Fig. S3).

To further address the importance of tumor cell BRAF^{V600E} and CDKN2A-RB status as key determinants of tumor response to these small molecule inhibitors, we treated mice with intracranial GS2 malignant astrocytomas, that are wild type for BRAF, express *p16^{Ink4a}*, but lack RB protein (Fig. S4), with mono- and combination therapies as before with the other tumor models. GS2 tumors showed no response to either inhibitor (Fig. 5 *E* and *F*), demonstrating specificity of responses to PLX4720 and PD0332991, respectively.

To gain insight into the additional benefit of PLX4720 and PD0332991, we analyzed the signaling pathway responses to monotherapies and combination therapy (Fig. S4). As expected, treatment of BRAF^{V600E} *CDKN2A*$^{-/-}$ cells with the CDK4/6 inhibitor PD0332991 reduced RB phosphorylation, and treatment with the BRAF inhibitor PLX4720 suppressed phosphorylation of extracellular signal-regulated kinase (ERK) and MAPK/ERK kinase (MEK). Surprisingly, however, treatment of BRAF^{V600E} *CDKN2A*$^{-/-}$ cell lines with PLX4720 alone resulted in elevated phosphorylation of the serine-threonine protein kinase AKT, which returned to basal level phosphorylation when cells were cotreated

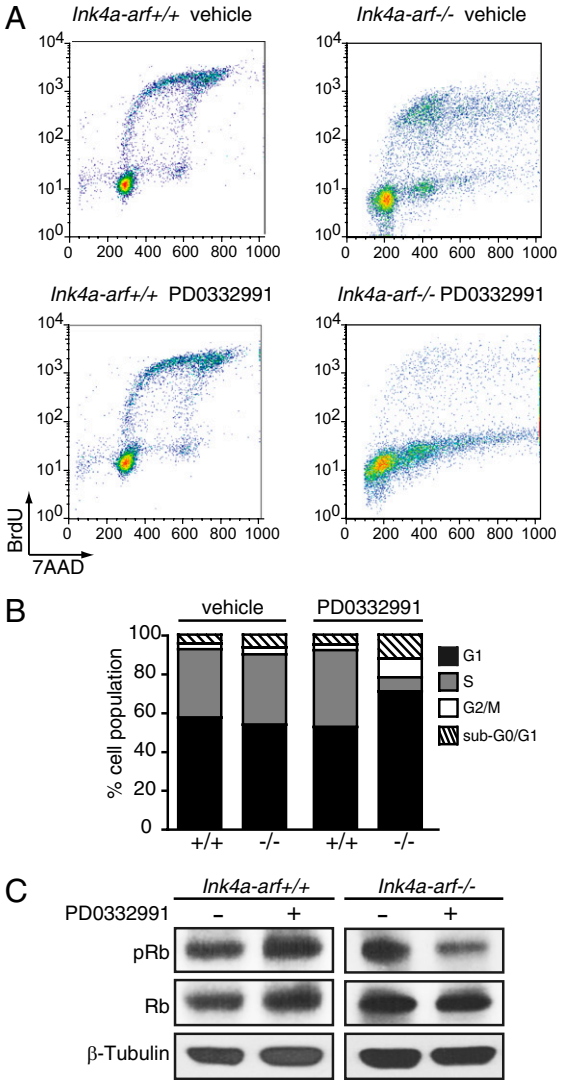

Fig. 3. CDK4/6 activity is required in the context of dual *BRAF*^{V600E}*; Ink4a-Arf*$^{-/-}$ genetic alterations for cell cycle progression in murine astrocytoma cells. *Braf*$^{CA/+}$*; Ink4a-Arf*$^{+/+}$ and *Braf*$^{CA/+}$*; Ink4a-Arf*$^{-/-}$ cells were incubated in the presence of vehicle (sodium lactate) or 10 μM PD0332991 for 48 h. (*A*) Flow cytometry analysis of treated *Braf*$^{CA/+}$*; Ink4a-Arf*$^{+/+}$ ($^{+/+}$) and *Braf*$^{CA/+}$*; Ink4a-Arf*$^{-/-}$ ($^{-/-}$) cells, pulsed with BrdU for 1 h and costained with FITC-conjugated BrdU and 7-amino-actinomycin D (7-AAD). The intensity of cell incorporated BrdU (logarithmic mode) vs. total DNA content with 7-AAD (linear signal amplification mode) is shown. (*B*) Cell cycle distribution of control and treated *Braf*$^{CA/+}$*; Ink4a-Arf*$^{+/+}$ ($^{+/+}$) and *Braf*$^{CA/+}$*; Ink4a-Arf*$^{-/-}$ ($^{-/-}$) cells. (*C*) Immunoblotting analysis of pRb and Rb in treated *Braf*$^{CA/+}$*; Ink4a-Arf*$^{+/+}$ and *Braf*$^{CA/+}$*; Ink4a-Arf*$^{-/-}$ cells.

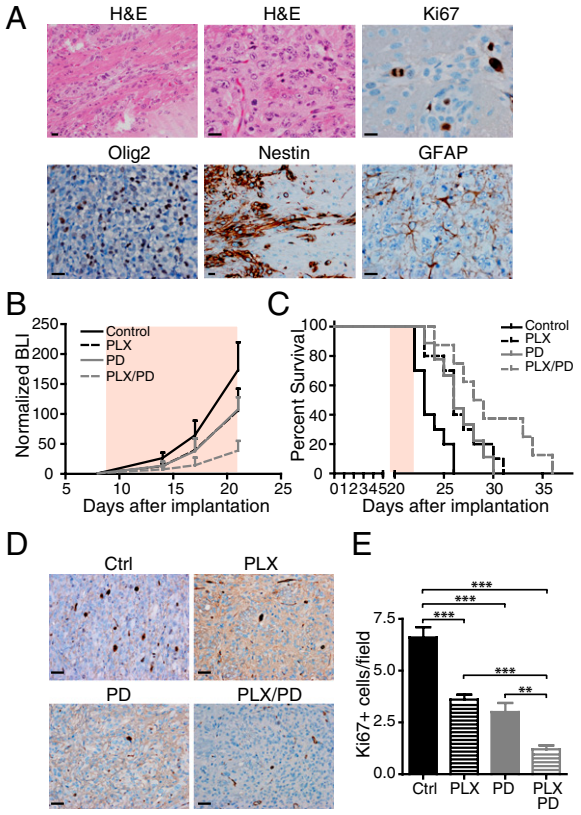

Fig. 4. Mono- and combination therapy of mice transduced with *Braf*$^{CA/+}$ *Ink4a-Arf*$^{-/-}$ murine cells using BRAF^{V600E} and CDK4/6 inhibitors. (*A*) Histological characterization of luciferase-modified *Braf*$^{CA/+}$ *Ink4a-Arf*$^{-/-}$ orthotopic allografts. (Scale bars, 20 μm.) (*B–E*) *Braf*$^{CA/+}$ *Ink4a-Arf*$^{-/-}$ orthotopic allografts were treated with PD0332991, PLX4720, or PLX4720 + PD0332991 for 14 consecutive days (pink area). (*B*) Bioluminescence imaging (BLI); P = 0.0110 for control vs. PLX + PD, P = 0.0341 for PLX vs. PLX + PD, P = 0.0222 for PD vs. PLX + PD. There are no statistically significant differences in tumor growth rate between control vs. PLX (P = 0.1866) or PD (P = 0.1971). (*C*) Kaplan–Meier survival curves; P = 0.0057 for control vs. PLX, P = 0.0069 for control vs. PD0332991, P = 0.0005 for control vs. PLX4720 + PD0332991. Although there is a trend for the combination being superior, there are no statistically significant differences in survival between PD or PLX vs. PD/PLX treatment groups: P = 0.0637 for combination vs. PLX only, and P = 0.0698 for combination vs. PD only. (*D*) Immunostaining of the proliferation marker Ki67 in control vs. treated (PLX, PD, and PLX/PD) tumors. (Scale bars, 20 μm.) (*E*) Quantification of the percentage of Ki67^{+} cells in untreated as well as treated tumor sections (mean ± SEM); ***P < 0.001, **P = 0.006.

with PD0332991. This unexpected result, showing combination treatment suppression of paradoxical stimulation of AKT by PLX4720 treatment alone, provides unique insight regarding the molecular basis of combination therapy antiproliferative effects on BRAF^{V600E} *CDKN2A*$^{-/-}$ tumors.

Discussion

Although malignant pediatric astrocytomas are particularly lethal CNS cancers, advances in therapy have been minimal, impaired by a poor grasp of the relevant underlying oncogenic signaling pathways. We have recently reported that ~20% of pediatric astrocytomas (WHO grades II–IV) carry the activating mutations in *BRAF*, which occurs commonly in combination with homozygous deletion of the *CDKN2A* locus, encoding *p19*^{ARF} and *p16*^{Ink4a} (11). Here we extend these findings by showing protumorigenic interactions of pathways regulated by BRAF^{V600E} and *p16*^{INK4A}.

Cooperative Interactions of *BRAF*^{V600E} Expression and *Ink4a-Arf* Loss of Function. Known *BRAF* alterations in human pilocytic astrocytomas include copy number gains, *BRAF-KIAA1549* fusion (13, 26–28), and the activating *BRAF*^{V600E} mutation (13). Combined expression of BRAF^{V600E} with silencing of *CDKN2A* has been observed in other cancers such as melanoma (29, 30). To investigate the relationship between *BRAF*^{V600E} and *Ink4a-Arf* deficiency in the development of malignant astrocytoma, we took advantage of a mouse model with a cre-conditional (floxed) allele of *Braf* in which the activating mutation is introduced in response to cre recombinase activity. This approach allows a precise recapitulation of BRAF^{V600E} expression by endogenous *cis*-acting regulatory sequences.

Although NP with heterozygous *BRAF*^{V600E} activation alone failed to form tumors after 6 mo postimplantation in SCID

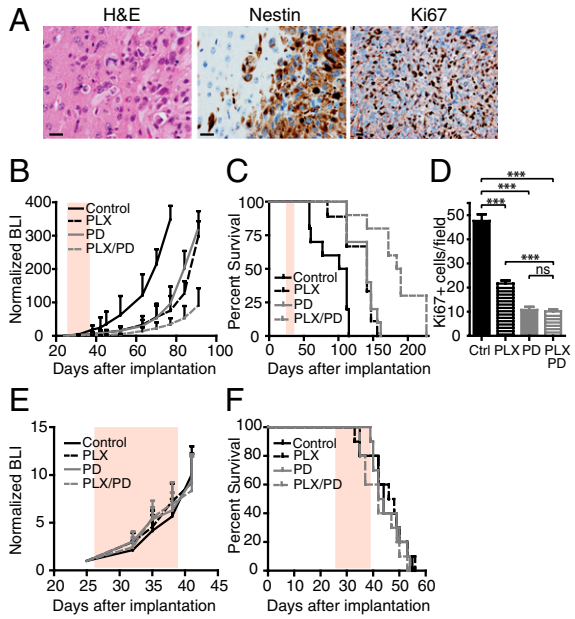

Fig. 5. Importance of $BRAF^{V600E}$ mutation and *Ink4a-Arf* deletion in determining orthotopic xenograft response to BRAF and CDK4/6 treatment. Tumors generated from the DBTRG05-MG astrocytoma line were treated with PD0332991, PLX4720, or PLX4720 + PD0332991 therapies for 14 consecutive days (pink area). (*A*) Histological features of DBTRG xenografts. (Scale bars, 20 μm.) (*B*) Bioluminescence imaging (BLI); $P = 0.0013$ for control vs. PLX, $P = 0.0120$ for control vs. PD, $P < 0.0001$ for control vs. PLX + PD combination therapy on day 77. $P = 0.0018$ for PLX vs. PLX + PD, $P = 0.0018$ for PD vs. PLX + PD. (*C*) Kaplan–Meier survival curves; $P = 0.0028$ for control vs. PLX, $P = 0.0005$ for control vs. PD0332991; $P < 0.001$ for PLX or PD vs. PLX4720 + PD0332991 combination therapy. (*D*) Quantification of the number of $Ki67^+$ cells in treated tumors (mean ± SEM); $^{***}P < 0.0001$; NS, not significant. (*E* and *F*) BLI and survival curves of mice transplanted with the GS2 astrocytoma line, which has wild-type BRAF and intact *Ink4a-Arf*.

recipient animals, it is possible that higher $BRAF^{V600E}$ expression levels might pass a tumorigenesis threshold. Indeed, overexpression of $BRAF^{V600E}$ using retrovirus, which might drive higher levels of BRAF activity or target higher numbers of suitable progenitors, is sufficient to produce pilocytic astrocytomas in mice (31).

In contrast, we found that heterozygous $BRAF^{V600E}$ expression combined with *Ink4-Arf* deficiency abrogated NP cell cycle arrest and conferred tumorgenicity to $BRAF^{V600E}$-expressing NPs when transplanted orthotopically into SCID mice or when activated in subventricular zone NP in situ. These results are consistent with observations reported in a recent study where $BRAF^{V600E}$ was overexpressed in *Ink4a-Arf*$^{-/-}$ neonatal brain using a retroviral vector (32) and indicate that the coincidence of *BRAF*-activating mutation and deletion of *CDKN2A* may represent obligatory steps during initiation and/or malignant progression of a subset of pediatric astrocytomas. One possibility is that $BRAF^{V600E}$ induces *p16* expression, promoting cell cycle arrest, as has been reported in human neural stem cells and v-raf-1 murine leukemia viral oncogene homolog 1 (RAF)-expressing human fibroblasts (33–35). From these data we conclude that expression of $BRAF^{V600E}$ triggers an oncogene-induced senescence-like (OIS) response, which is mediated by elevated p16 expression (Fig. S5). If so, when $BRAF^{V600E}$ expression is triggered in *Ink4a-Arf* deficient cells there is no OIS and tumor progression is permitted.

Our previously published survey of gene alterations in diffuse pediatric astrocytomas, which included analysis of tumor copy number variation as well as investigation of selected cancer-associated genes, such as *BRAF* and *P53*, revealed no other gene alteration with $BRAF^{T1799A}$ other than homozygous *CDKN2A* deletions (11). In addition, the DBTRG05-MG and AM-38 astrocytoma lines that we used here do not carry additional alterations other than *PTEN* inactivation in DBTRG05-MG (25). These results do not exclude the possibility of other gene alterations acting in combination with $BRAF^{V600E}$ to promote tumorigenesis, such as the missense mutation of histone H3.3 encoding H3F3A, which has been reported in a significant proportion of pediatric GBMs (6, 7), but the results do support *CDKN2A* inactivation as being especially effective in cooperating with $BRAF^{V600E}$ for promoting tumor development.

We noted that hGFAP-cre; $BRAF^{V600E}$; *Ink4a-Arf*$^{-/-}$ mouse-derived astrocytomas initially showed a propensity for exophytic growth. Interestingly, in a recent study (13), $BRAF^{V600E}$ mutations have been associated with pleomorphic xanthoastrocytoma (PXA), a superficial human astrocytic tumor that can grow exophytically. Although this study did not address *CDKN2A* status, deletion of *CDKN2A* has independently been identified in pediatric pleomorphic xanthoastrocytomas (36–38). Future work is needed to determine whether the $BRAF^{V600E}$, *p16*-deficient astrocytomas we describe may initially be tropic for superficial growth.

Combinatorial Therapy May Be Efficacious for a Genetic Subset of Pediatric Astrocytomas. The finding of cooperativity between $BRAF^{V600E}$ activation and *Ink4a-Arf* deficiency in murine and human cells has therapeutic implications; namely, that combined inhibition of CDK4/6 and $BRAF^{V600E}$ could prove efficacious in treating malignant astrocytomas with these gene alterations. In the present study, we found that both murine and human $BRAF^{V600E}$ mutant, *Ink4a-Arf*–deficient astrocytomas respond to the $BRAF^{V600E}$ inhibitor PLX4720, as indicated by a reduced rate of intracranial tumor growth and extended survival. These results are consistent with our previous report using PLX4720 to inhibit RAF activity in nonpediatric astrocytoma models (39) and suggest that PLX4720 has a favorable biodistribution for use in treating $BRAF^{V600E}$-driven brain cancers. Importantly, when we combined PLX4720 with the CDK4/6 inhibitor PD0332991, we observed additive antitumor effects. Our report uniquely indicates that the two inhibitors can be used in combination for increasing antitumor effect, due to therapeutic targeting of distinct enzymatic activities. Interestingly, the paradoxical increase in AKT phosphorylation following PLX4720 treatment can be reversed by cotreatment with PD0332991. This result lends further support to the use of combination therapy for treating $BRAF^{V600E}$ and CDKN2A-deficient tumors. Taken together, our data support the importance of tumor genotype for predicting response to each therapy, used singularly or in combination. We note that no animal subjects with intracranial $BRAF^{V600E}$-*p16* null tumors, from any of the three in vivo efficacy experiments (Figs. 4 and 5 and Fig. S3), died while receiving combination therapy. This observation raises the question of how long survival can be extended by continuous combination therapy, and related studies are underway to address this question.

Appropriate genetic diagnostic tests are available for identifying tumors with *BRAF* mutation and also lacking *CDKN2A*, and their routine application to pediatric and adult malignant astrocytomas would reliably identify patients who might benefit from this combination therapy. The frequency of $BRAF^{V600E}$ mutations in pediatric glioblastomas is estimated between 6 and 18% (11, 13), whereas the frequency in adult glioblastomas is estimated to be 1–3% (13, 40). In pediatric anaplastic astrocytomas (WHO grade III), we found $BRAF^{V600E}$ in 3 of 23 cases (13%, ref. 39). The frequency of $BRAF^{V600E}$ in pediatric grade III astrocytomas has not been published by others. For adult anaplastic astrocytomas, no instances of V600E were determined among 51 cases. In total, these results suggest that $BRAF^{V600E}$ occurs at a significant frequency among WHO grade III and grade IV pediatric astrocytomas, but is rare among corresponding adult tumors.

Our data, although suggestive, need to be further examined in a preclinical setting to address length of benefit from this

therapy, as well as possible tumor adaptation to therapy. Nonetheless, our preliminary results are promising for this approach providing effective treatment for appropriately diagnosed CNS cancer patients.

Materials and Methods

Neural Progenitor and Glioblastoma Cultures. Mouse neurosphere cultures were established from E14.5 basal progenitors, as previously described (20), with the modification that cells were grown in the presence of EGF and basic FGF (20 ng/mL each). AM-38 human glioblastoma cells were obtained from the Japan Health Sciences Foundation Health Science Research Resources Bank; DBTRG05-MG human glioblastoma cells were obtained from the American Type Culture Collection. Cells were propagated in Eagle's MEM supplemented with 10% FBS and nonessential amino acids. GS2 cells were obtained from Manfred Westphal, University Hospital Eppendorf, Hamburg, Germany, and maintained as neurosphere cultures, as previously described (41).

Intracranial Injections of Tumor Cells and Cre-Expressing Adenovirus. Tumor cells were transplanted into the brains of SCID mice (ICRSC-M; Taconic) as previously described (20), at the following coordinates, according to Bregma: 1.0 mm (anterior), 2.0 mm (lateral), and 3.0 mm (deep). Alternatively, cells were transplanted into athymic mice (5-wk-old female, nu/nu genotype, BALB/c background; Simonsen Laboratories) as previously described (42). $Braf^{CA/+}$ and $Braf^{CA/+}$ $Ink4a\text{-}arf^{fl/fl}$ 60-d-old mice were injected with 2 μL of adenovirus (10^9 multiplicity of infection, MOI) in which cre recombinase expression is regulated by a ubiquitous promoter (Vector Biolabs). The following coordinates, according to Bregma, were used: 1.0 mm (anterior), 1.0 mm (lateral), and 1.8 mm (deep).

Treatment of Tumor-Bearing Athymic Mice with $BRAF^{V600E}$ and CDK4/6 Inhibitors. Athymic mice transplanted with luciferase-modified 10776, DBTRG05-MG, or AM-38 cell lines were randomly assigned to vehicle control (DMSO or 50 mM sodium lactate, pH 4, for PLX or PD0332991, respectively), PLX treatment (PLX4720; Plexxikon), PD treatment (PD0332991, Pfizer), or a combination of PLX and PD treatments. The treatment group received a daily dose of 10 mg/kg of PLX by i.p. injection and/or oral administration of 150 mg/kg of PD for 14 consecutive days. All mice were monitored every day for the development of symptoms related to tumor growth and twice weekly by BLI. Mice were killed when they exhibited symptoms indicative of significant impairment to neurological function.

ACKNOWLEDGMENTS. The authors thank Maxwell W. Tom and Sista Sugiarto for technical assistance, Ron DePinho for providing the $Ink4a\text{-}Arf^{lox/lox}$ mouse line, Peter Hirth and Brian West (Plexxikon) for providing PLX4720, and Pfizer for providing PD0332991. The authors acknowledge support from the Pediatric Brain Tumor Foundation, the Pediatric Low-Grade Astrocytoma Foundation, the Rally Foundation for Childhood Cancer Research, the Campini Foundation, the McDonnell Foundation, the Clinical and Translational Science Institute, the University of California at San Francisco, the American Association for Cancer Research/National Brain Tumor Society (R.A.I.), the American Brain Tumor Association (A.G.), and National Institutes of Health Grants K08NS065268 (to T.N.), 5K08NS063456 (to J.J.P.), R01CA159467 (to T.W. and C.D.J.), R01CA131261 (to M.M), 1RO1CA164746 (to C.P.), CA097257 (to W.A.W, C.P., and C.D.J.), R01 NS040511 (to D.H.R.), and 2R01NS057727-05 (to D.H.R). D.H.R. is a Howard Hughes Medical Institute Investigator.

1. Central Brain Tumor Registry of the United States (2004–2007) Primary Brain and Central Nervous System Tumors Diagnosed in the United States in 2004–2007, Statistical Report. Available at http://www.cbtrus.org/reports/reports.html. Accessed September 11, 2011.
2. Phillips HS, et al.; (2006) Molecular subclasses of high-grade glioma predict prognosis, delineate a pattern of disease progression, and resemble stages in neurogenesis. *Cancer Cell* 9:157–173.
3. Verhaak RG, et al.; Cancer Genome Atlas Research Network (2010) Integrated genomic analysis identifies clinically relevant subtypes of glioblastoma characterized by abnormalities in PDGFRA, IDH1, EGFR, and NF1. *Cancer Cell* 17:98–110.
4. Brennan C, et al. (2009) Glioblastoma subclasses can be defined by activity among signal transduction pathways and associated genomic alterations. *PLoS ONE* 4:e7752.
5. Bax DA, et al. (2010) A distinct spectrum of copy number aberrations in pediatric high-grade gliomas. *Clin Cancer Res* 16:3368–3377.
6. Wu G, et al.; St. Jude Children's Research Hospital–Washington University Pediatric Cancer Genome Project (2012) Somatic histone H3 alterations in pediatric diffuse intrinsic pontine gliomas and non-brainstem glioblastomas. *Nat Genet* 44:251–253.
7. Schwartzentruber J, et al. (2012) Driver mutations in histone H3.3 and chromatin remodelling genes in paediatric glioblastoma. *Nature* 482:226–231.
8. Liang ML, et al. (2008) Tyrosine kinase expression in pediatric high grade astrocytoma. *J Neurooncol* 87:247–253.
9. Paugh BS, et al. (2010) Integrated molecular genetic profiling of pediatric high-grade gliomas reveals key differences with the adult disease. *J Clin Oncol* 28:3061–3068.
10. Pollack IF, et al.; Children's Oncology Group (2006) Rarity of PTEN deletions and EGFR amplification in malignant gliomas of childhood: Results from the Children's Cancer Group 945 cohort. *J Neurosurg* 105(5, Suppl):418–424.
11. Schiffman JD, et al. (2010) Oncogenic BRAF mutation with CDKN2A inactivation is characteristic of a subset of pediatric malignant astrocytomas. *Cancer Res* 70:512–519.
12. Dias-Santagata D, et al. (2011) BRAF V600E mutations are common in pleomorphic xanthoastrocytoma: Diagnostic and therapeutic implications. *PLoS ONE* 6:e17948.
13. Schindler G, et al. (2011) Analysis of BRAF V600E mutation in 1,320 nervous system tumors reveals high mutation frequencies in pleomorphic xanthoastrocytoma, ganglioglioma and extra-cerebellar pilocytic astrocytoma. *Acta Neuropathol* 121: 397–405.
14. Dankort D, et al. (2007) A new mouse model to explore the initiation, progression, and therapy of BRAFV600E-induced lung tumors. *Genes Dev* 21:379–384.
15. Corcoran RB, et al. (2010) BRAF gene amplification can promote acquired resistance to MEK inhibitors in cancer cells harboring the BRAF V600E mutation. *Sci Signal* 3:ra84.
16. Dankort D, et al. (2009) Braf(V600E) cooperates with Pten loss to induce metastatic melanoma. *Nat Genet* 41:544–552.
17. Charles RP, Iezza G, Amendola E, Dankort D, McMahon M (2011) Mutationally activated BRAF(V600E) elicits papillary thyroid cancer in the adult mouse. *Cancer Res* 71: 3863–3871.
18. Brenner M, Kisseberth WC, Su Y, Besnard F, Messing A (1994) GFAP promoter directs astrocyte-specific expression in transgenic mice. *J Neurosci* 14:1030–1037.
19. Bachoo RM, et al. (2002) Epidermal growth factor receptor and Ink4a/Arf: Convergent mechanisms governing terminal differentiation and transformation along the neural stem cell to astrocyte axis. *Cancer Cell* 1:269–277.
20. Ligon KL, et al. (2007) Olig2-regulated lineage-restricted pathway controls replication competence in neural stem cells and malignant glioma. *Neuron* 53:503–517.
21. Otero JJ, Rowitch D, Vandenberg S (2010) OLIG2 is differentially expressed in pediatric astrocytic and in ependymal neoplasms. *J Neurooncol* 104:423–438.
22. National Institutes of Health Registry of Clinical Trials Website. Available at http://clinicaltrials.gov/ct2/results?term=pd-0332991. Accessed August 23, 2011.
23. Smalley KS (2010) PLX-4032, a small-molecule B-Raf inhibitor for the potential treatment of malignant melanoma. *Curr Opin Investig Drugs* 11:699–706.
24. Davies H, et al. (2002) Mutations of the BRAF gene in human cancer. *Nature* 417: 949–954.
25. Michaud K, et al. (2010) Pharmacologic inhibition of cyclin-dependent kinases 4 and 6 arrests the growth of glioblastoma multiforme intracranial xenografts. *Cancer Res* 70: 3228–3238.
26. Jones DT, et al. (2008) Tandem duplication producing a novel oncogenic BRAF fusion gene defines the majority of pilocytic astrocytomas. *Cancer Res* 68:8673–8677.
27. Korshunov A, et al. (2009) Combined molecular analysis of BRAF and IDH1 distinguishes pilocytic astrocytoma from diffuse astrocytoma. *Acta Neuropathol* 118: 401–405.
28. Pfister S, et al. (2008) BRAF gene duplication constitutes a mechanism of MAPK pathway activation in low-grade astrocytomas. *J Clin Invest* 118:1739–1749.
29. Dhomen N, et al. (2009) Oncogenic Braf induces melanocyte senescence and melanoma in mice. *Cancer Cell* 15:294–303.
30. Garraway LA, et al. (2005) Integrative genomic analyses identify MITF as a lineage survival oncogene amplified in malignant melanoma. *Nature* 436:117–122.
31. Gronych J, et al. (2011) An activated mutant BRAF kinase domain is sufficient to induce pilocytic astrocytoma in mice. *J Clin Invest* 121:1344–1348.
32. Robinson JP, et al. (2010) Activated BRAF induces gliomas in mice when combined with Ink4a/Arf loss or Akt activation. *Oncogene* 29:335–344.
33. Michaloglou C, et al. (2005) BRAFE600-associated senescence-like cell cycle arrest of human naevi. *Nature* 436:720–724.
34. Raabe EH, et al. (2011) BRAF activation induces transformation and then senescence in human neural stem cells: A pilocytic astrocytoma model. *Clin Cancer Res* 17: 3590–3599.
35. Zhu J, Woods D, McMahon M, Bishop JM (1998) Senescence of human fibroblasts induced by oncogenic Raf. *Genes Dev* 12:2997–3007.
36. Dougherty MJ, et al. (2010) Activating mutations in BRAF characterize a spectrum of pediatric low-grade gliomas. *Neuro-oncol* 12:621–630, 10.1093/neuonc/noq007.
37. Forshew T, et al. (2009) Activation of the ERK/MAPK pathway: A signature genetic defect in posterior fossa pilocytic astrocytomas. *J Pathol* 218:172–181.
38. Weber RG, et al. (2007) Frequent loss of chromosome 9, homozygous CDKN2A/p14 (ARF)/CDKN2B deletion and low TSC1 mRNA expression in pleomorphic xanthoastrocytomas. *Oncogene* 26:1088–1097.
39. Nicolaides TP, et al. (2011) Targeted therapy for BRAFV600E malignant astrocytoma. *Clin Cancer Res* 17:7595–7604.
40. Knobbe CB, Reifenberger J, Reifenberger G (2004) Mutation analysis of the Ras pathway genes NRAS, HRAS, KRAS and BRAF in glioblastomas. *Acta Neuropathol* 108: 467–470.
41. Günther HS, et al. (2008) Glioblastoma-derived stem cell-enriched cultures form distinct subgroups according to molecular and phenotypic criteria. *Oncogene* 27: 2897–2909.
42. Hashizume R, et al. (2010) Morphologic and molecular characterization of ATRT xenografts adapted for orthotopic therapeutic testing. *Neuro-oncol* 12:366–376.